

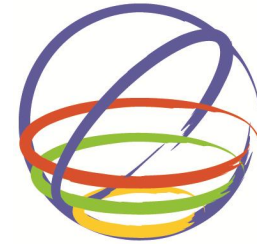
# THREE-DIMENSIONAL SOIL-STRUCTURE INTERACTION ANALYSIS OF CUT-AND-COVER TUNNELS

**R. Donikian, & C. Liu**

*Parsons Brinckerhoff, San Francisco, CA, USA*

**Q. Liu, & K. Clinch**

*Arup North America, San Francisco, CA, USA*



**15 WCEE**  
LISBOA 2012

## SUMMARY:

The paper highlights the significant aspects of seismic performance assessments of cut-and-cover tunnels situated in high seismic zones, based on three-dimensional (3D) dynamic soil-structure interaction (SSI) analyses. Presented are key features from a case study performed for the ‘Phase 1’ Design Development stage of the Doyle Drive Reconstruction Project, San Francisco, California, USA, where a 3D model of a 1,000-ft long, curved, cut-and-cover tunnel (under construction) and its future adjacent twin was developed. The SASSI2000 computer program was used for 3D SSI analyses of the twin-tunnel system, based on simulated ground motions characteristic of seismic P- and S-waves. The paper highlights key aspects of the soil-structure system parameters, response quantities, and performance measures underlying the Performance Based Earthquake Engineering (PBEE) design approach. The significance of 3D SSI models for global dynamic response assessments of shallow, large-scale, cut-and-cover tunnels that capture kinematic and inertial interaction effects is also discussed.

*Keywords: soil-structure interaction; cut-and-cover tunnel; tunnel racking; PBEE*

## 1. INTRODUCTION

The paper focuses on the merits of using three-dimensional soil-structure-interaction analyses for the seismic design and performance evaluation of large-scale, shallow, cut-and-cover tunnels situated in high seismic risk zones. Insights obtained from case studies performed for the seismic design of a 1,000-ft long, 60-ft wide, curved, concrete cut-and-cover tunnel as part of the Phase 1 project development of the Doyle Drive Reconstruction Project (renamed to the Presidio Parkway Project) are discussed. The project site is located in the Presidio of San Francisco, California, USA; the renderings in Figures 1.1 and 1.2 depict the project alignment and the tunnels. The characteristics of the 3D SSI model of the tunnel (Southbound Battery Tunnel) currently under construction –including the planned future adjacent twin tunnel (Northbound Battery Tunnel) shown in Figure 1.1– generated to study the overall response subjected to vibratory strong ground motions are discussed in the paper. The frequency-domain based, hybrid “soil half-space/finite element structure”, computer program SASSI2000 (Ostadan, 2006) was used for the analyses of the twin-tunnel system.

The paper highlights key aspects of: (a) soil-structure system parameters including soil medium dilatational P-wave and shear S-wave (SV and SH) velocity profiles, transfer functions, ‘equivalent linearization’ of soil and structure properties; (b) response quantities including acceleration, displacement, racking deformations, and stresses & strains in tunnel linings; and (c) performance measures underlying the Performance Based Earthquake Engineering design approach adopted.

The significance of using 3D models to assess the global dynamic response of shallow, large-scale, cut-and-cover tunnels based on tractable dynamic SSI models that properly capture kinematic and inertial interaction effects is also discussed.



**Figure 1.1.** Renderings of Battery Tunnels in the future Presidio Parkway of San Francisco, CA



**Figure 1.2.** Alignment of future Presidio Parkway, San Francisco, CA

## 2. SEISMIC PERFORMANCE EVALUATION MEASURES

The state-of-the-practice procedure for the seismic design of underground structures entails the ground deformation approach (quasi-static deformations) as well as the consideration of soil-structure interaction effects (dynamic loading). For tunnels embedded in rock or into deep stiff soil layers the design is generally controlled by quasi-static deformations of the surrounding ground, since the geologic medium is much stiffer than the tunnel lining. In this case study, where the tunnel structure is stiff relative to the surrounding soil, and it is embedded in a shallow medium/stiff soil site, the effects of SSI become significant. The components of the PBEE design approach taken in the study included: site-specific seismic hazard assessment; establishment of design and performance criteria; selection of performance measures; and the application of appropriate structural analysis methods.

### 2.1. Seismic Hazard and Ground Motions

#### 2.1.1. Seismic Loading & Performance Requirements

The project design criteria are based on a two-level seismic performance requirement characterised by *Functionality* and *Safety* Evaluation events, the FEE and SEE, respectively. The SEE is representative of a  $M_w$ 7.5 event with a 1,000-year return period, and the FEE is representative of a  $M_w$ 6.9 event with a 108-year return period. The associated performance levels established are ‘Serviceable/Repairable Damage’ for the FEE, and ‘No-Collapse/Repairable Damage’ for the SEE. A probabilistic site-specific

hazard assessment was performed based on the Next Generation Attenuation (NGA) model, and horizontal and vertical design acceleration spectra, shown in Figure 2.1, were developed corresponding to an average shear wave velocity site characterization index of  $V_{s30} = 3,000$  ft/sec. Three-component, spectrum-compatible motions were developed corresponding to Fault-Parallel (FP), Fault-Normal (FN), and Vertical (V) components of motions at rock, based on recorded motions as seed time-histories (the Manjil, Kocaeli, & Chi-Chi records in the NGA database were used for SEE).

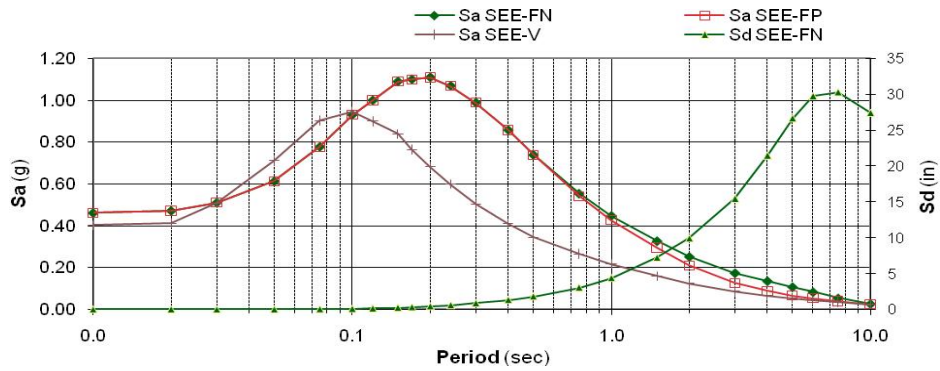


**Figure 2.1.** SEE Design response spectra,  $V_{s30} = 3,000$  fps, 5% spectral damping

*2.1.2. Site Response Analyses, Free-Field Motions, and Strain-compatible Vs Profiles*

Site response analyses performed to obtain the free-field motions and strain-compatible profiles needed for the SSI analyses were based on soil profiles such as the one shown in Figure 2.2. The depth-variable free-field accelerations and corresponding response spectra for the east end of the tunnel are shown in Figure 2.3. The strain-compatible shear-wave velocity and soil damping profiles are shown in Figure 2.4, corresponding to the ‘deep’ and ‘shallow’ soil profiles at the east and west ends of the tunnel, respectively.

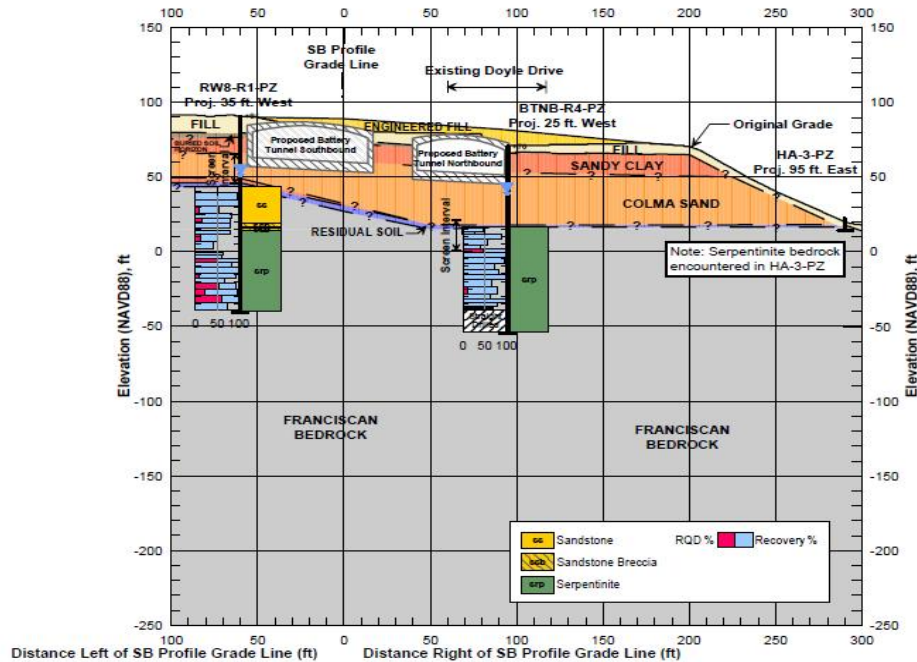


**Figure 2.2.** Typical soil profile at east end of tunnel footprint

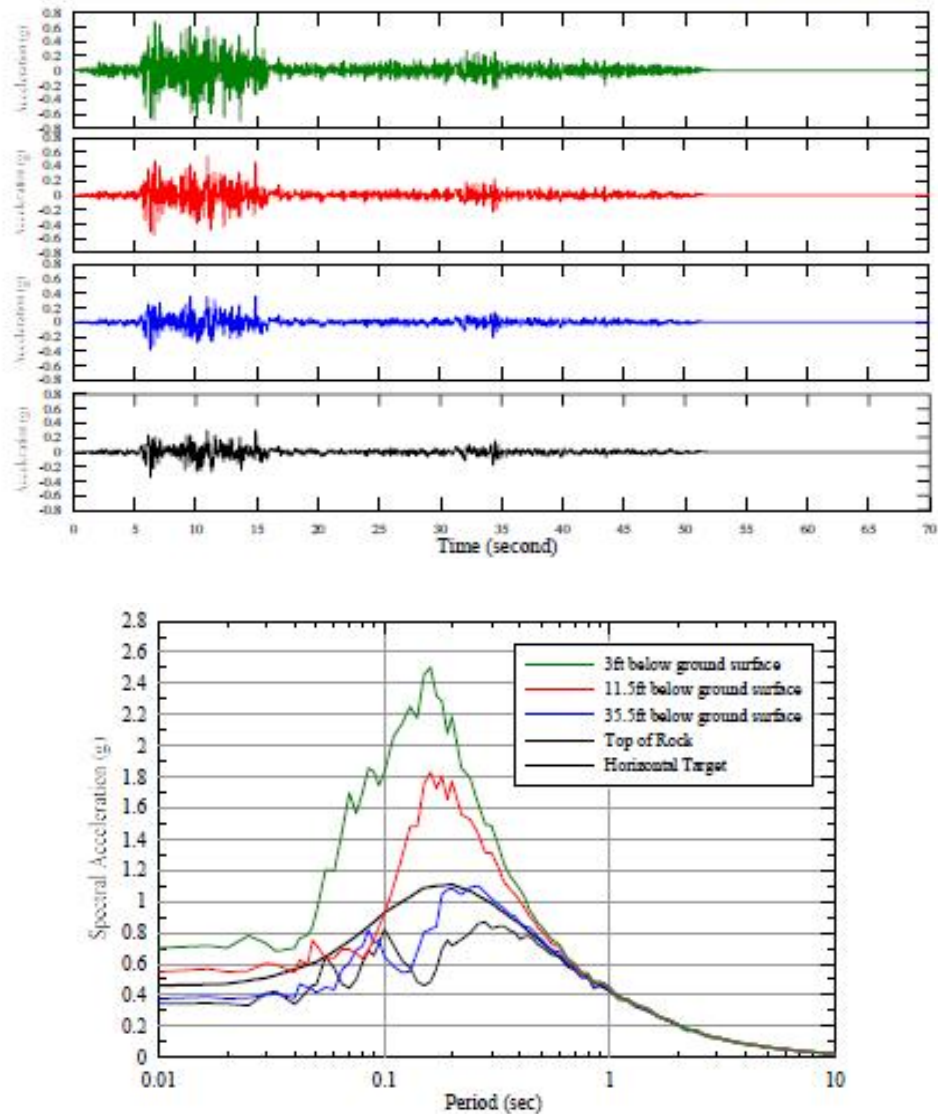


**Figure 2.3.** Depth-variable free-field accelerations & corresponding spectra (5% damping) for Manjil-based SEE

## 2.2. Structural Performance

### 2.2.1. Ductility & Strength Measures

The primary seismic structural performance measure for tunnels is the transverse ‘racking distortion’ of the cross-section, and it involves the establishment of target values of deformation ductility ( $\mu$ ) defined (conventionally) by:  $\mu_{FEE} = \delta_{FEE} / \delta_y$  and  $\mu_{SEE} = \delta_{SEE} / \delta_y$ , where  $\delta_y$  is the ‘yield limit state’ deformation, and  $\delta_{FEE}$  &  $\delta_{SEE}$  are the ‘ultimate limit state’ deformations for the SEE and FEE levels, respectively. These measures are governed by material strain limits established by the structural design criteria; in this case, the target ductilities specified were 4 and 2, corresponding to the SEE and FEE performance levels, respectively. In order to maintain structural stability in the primary vertical load carrying members of the tunnel and accommodate deformations in the inelastic range of the structural components, flexural strength measures are required. In terms of the 3D global behaviour of the tunnel, these strength measures pertain to capacities of the tunnel cross-section for resisting transverse and vertical shears, vertical and transverse bending, and axial forces. For the lateral racking capacity of the tunnel cross-section, the plastic shear capacity of the walls is fundamental for strength, since it ensures the formation of controlled plastic hinging in the tunnel walls.

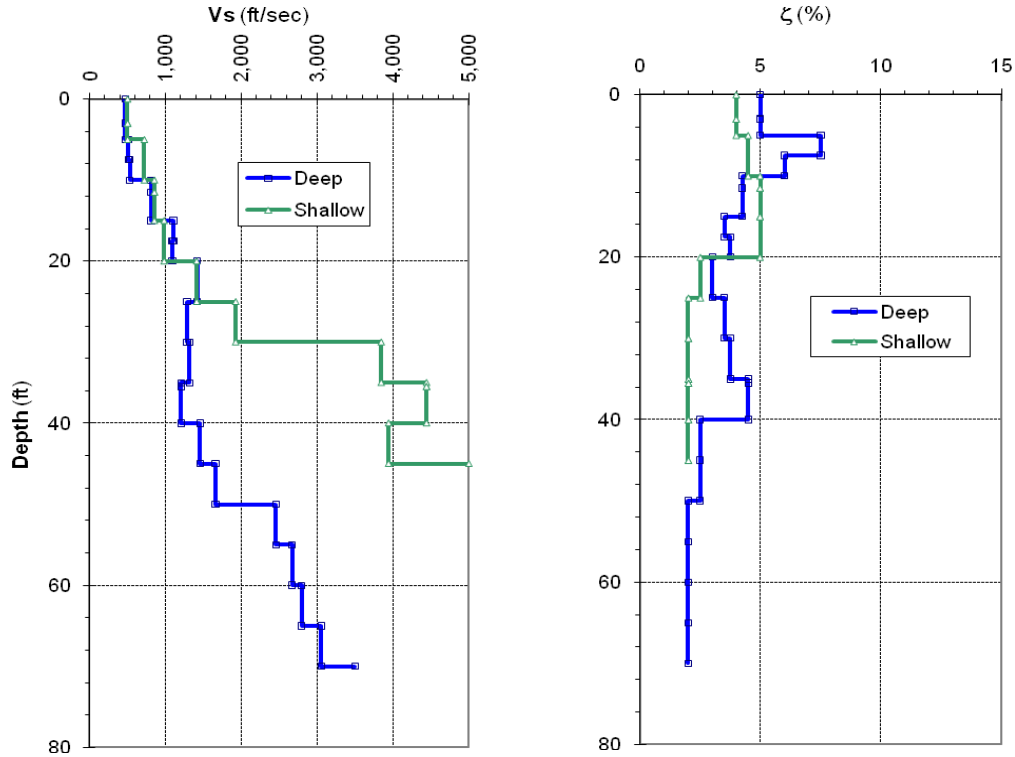


**Figure 2.4.** Strain-compatible shear-wave velocity and damping profiles

### 2.2.2. Structural Capacity

Capacities of tunnel flexural members and cross-section racking distortion performance measures were established by means of one-dimensional (1D) and two-dimensional (2D) local models, including: (a) moment-curvature analyses of the tunnel wall, roof, and invert unit strip cross-sections to develop inelastic material properties for push-over analyses and P-M (axial force – bending moment) interaction curves; (b) static, displacement controlled push-over analyses of the tunnel lining surrounded by soil springs (vertical sub-grade reactions and horizontal soil springs) using inelastic finite-element models utilizing the ADINA computer program (ADINA R&D, Inc., 2005), to obtain load-deflection curves of tunnel cross-section racking behavior for the assessment of ductility capacities; and (c) calculations for establishing shear strengths of flexural members.

### 2.2.3. Seismic Demand

The estimation of the seismic demand on the large-scale cut-and-cover tunnel under study involved a progressive approach: (a) beginning with simplified manual racking analyses, based on free-field racking drifts (obtained from the site response analyses) and Racking Ratio,  $R$ , obtained from ‘Racking–Flexibility Ratio’ curves (Penzien, J., 2000), which is a function of the ratio of the tunnel lining flexibility to the excavated soil plug flexibility under shearing deformation; (b) transitioning to 2D parametric SSI analyses using the SASSI2000 and FLAC computer programs (Itasca Consulting Group, 1998); and (c) performing 3D SSI analyses using SASSI2000, the central topic of this paper.

## 3. SOIL-STRUCTURE INTERACTION ANALYSES

The principal goal of performing 3D SSI analyses for this large-scale twin-tunnel system was to obtain a rational seismic demand estimate on the global system as whole. The 3D SASSI2000 model developed for this investigation, depicted in Figure 3.1, includes the curved alignment and cross-section geometry of the tunnel, influence of the adjacent future tunnel, and wave passage/incoherency effects of the seismic input motions simulated by inclined SV-waves.

#### Model Characteristics

- 36,639 Dynamic DOF
- 10,602 Impedance/ Interaction DOF

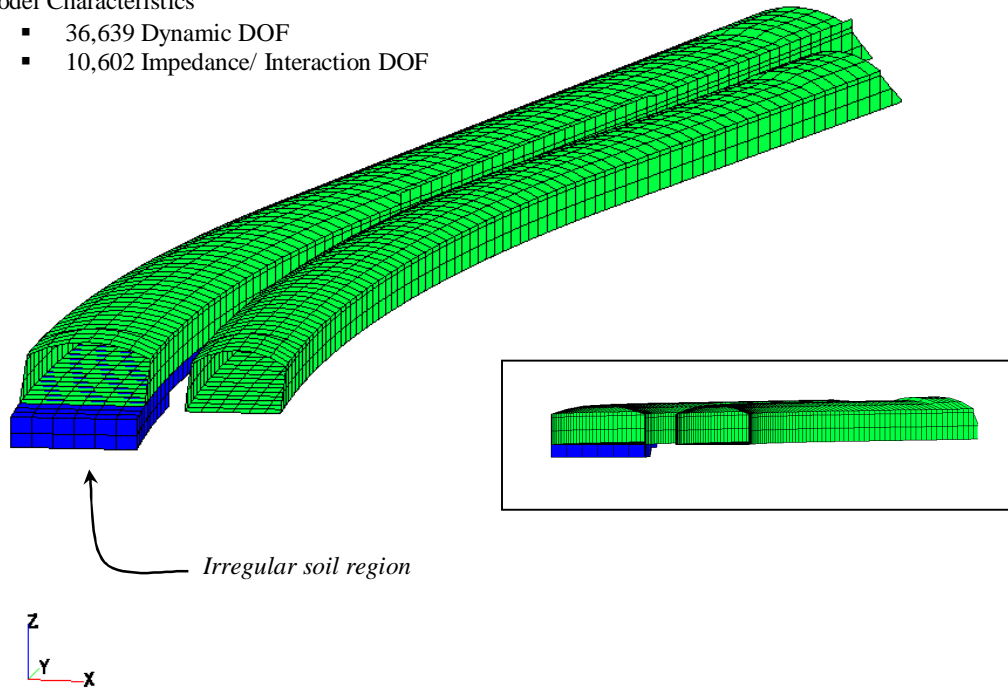


Figure 3.1. 3D SASSI2000 model of Battery Tunnels

### 3.1. SASSI2000 Model Characteristics

The SASSI2000 computer program, based on a mathematical sub-structuring formulation in the frequency domain, is an efficient analytical tool that uses impedance matrices for the dynamic response computation of complex linear soil-structure systems. Dynamic response is computed by Transfer Functions between the (input) seismic excitation (acceleration ‘control motion’) and (output) response quantities of interest. For underground structures the effects of far-field soil non-linearities and structural non-linearities may reasonably be accounted for by equivalent linearization. Relevant characteristics of the 3D SASSI2000 model of the case study and the assumptions made in developing it are summarized below.

#### 3.1.1. Soil-Structure System Model

The tunnel walls, roof, and invert slabs are modelled with 3D PLATE/SHELL finite elements, with appropriately factored concrete material elastic moduli to simulate effective stiffness properties (obtained from moment-curvature analyses). The geologic medium (treated as a horizontally layered half-space) was modelled using the shallow soil profile of the alignment shown in Figure 2.4, representative of most of the tunnel alignment profile beginning from the west end. It consists of 39 layers of soil above the elastic half-space, characterized by the strain-compatible shear-wave velocity and damping profiles shown in Figure 2.4. The dilatational P-wave velocity profile required to capture vertical response was derived from small-strain soil parameters. (Note: the strain-compatible profiles involve equivalent linearization of the far-field soil profile).

#### 3.1.2. Irregular Soil Regions

To account for the soil profile variation along the tunnel, i.e., the ‘deep’ profile shown in Figure 2.4, the ‘irregular soil region’ at the east end of the tunnel shown in Figure 3.1 was introduced using 3D SOLID structural elements with the properties of the thicker soft soil layers. A separate study was conducted to evaluate the effectiveness of this approach using three different 2D models to compare the free-field response of: the deep profile; the shallow profile; and the modified shallow profile with the irregular zone. The results indicated that this approach provides a reasonable approximation.

### 3.1.3. Control Motions

The seismic input ‘control motion’ applied for each mutually orthogonal direction of loading (longitudinal, transverse, and vertical) consists of a free-field ‘interface’ acceleration time-history (see sample in Figure 2.3) corresponding to any appropriate soil layer in the profile (e.g., elevation of invert slab). The tri-axial set of control motions representative of the SEE in the shallow profile was used to simulate vertically propagating SH-waves in the transverse direction and P-waves in the vertical direction, and inclined SV-waves propagating in the vertical plane at an incidence angle of 21.5 degrees (with respect to the vertical axis) to simulate the wave-passage/incoherency effect (note that this generates refracted P-waves in the system).

### 3.1.4. Analysis Parameters

The analytical options and parameters used entail: (a) the Subtraction Method to model the soil-structure system with 10,600 ‘interaction’ degrees-of-freedom for the impedance calculation; (b) highest analysis frequencies of 20 Hz for horizontal response (29 frequencies to anchor transfer functions), and 42 Hz for vertical response (31 frequencies to anchor transfer function); and (c) 80-second duration using a time step size of 0.01 seconds. The appropriate maximum element mesh size required to satisfy the cut-off frequency criterion ( $h_{elem} < \lambda/5$ ;  $\lambda = V_s/f$ ) appropriate for this scale model was determined to be approximately 10-ft by parametric 2D analyses (Liu, C. et al, 2012).

### 3.1.5. Transfer Functions

The transfer functions for transverse acceleration, with respect to the control motion applied at rock elevation, at the free-field and at the centre of the tunnel are shown in Figure 3.2. The free-field soil response (monitored by a vertical string of ‘interaction nodes’ located 500-ft away from the structure) is dominated by a 0.11 sec vibration period ( $f = 9.1$  Hz), while the soil-structure system introduces a vibration period of 0.19 sec ( $f = 5.26$  Hz) that governs the transverse acceleration response of the tunnel crown. This longer period component has a much broader band than the free-field soil column.

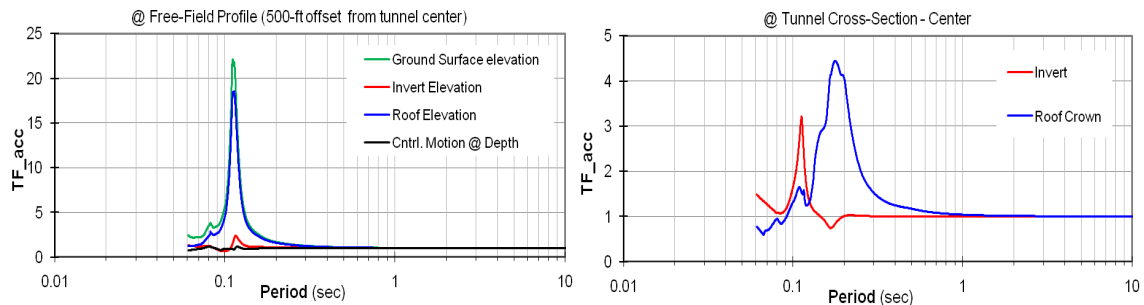


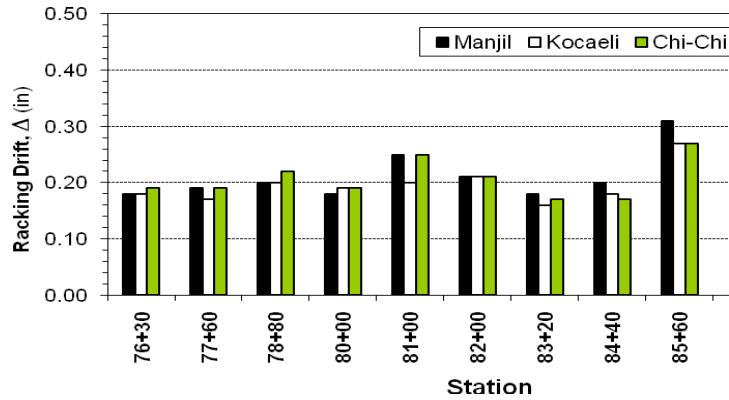
**Figure 3.2.** 3D SASSI2000 Model transfer functions for acceleration – Transverse Direction

## 3.2. SASSI2000 3D Model Response Evaluation Summary

The response quantities of interest extracted from the 3D analyses discussed in this paper include: (a) distribution of the transverse racking drift demand along the tunnel alignment; (b) stresses and strains in the tunnel lining induced by axial extension/compression, vertical & transverse bending of the tunnel lining; and (c) shear stress distributions on the tunnel lining due to transverse & vertical shear and torsion on the cross-section.

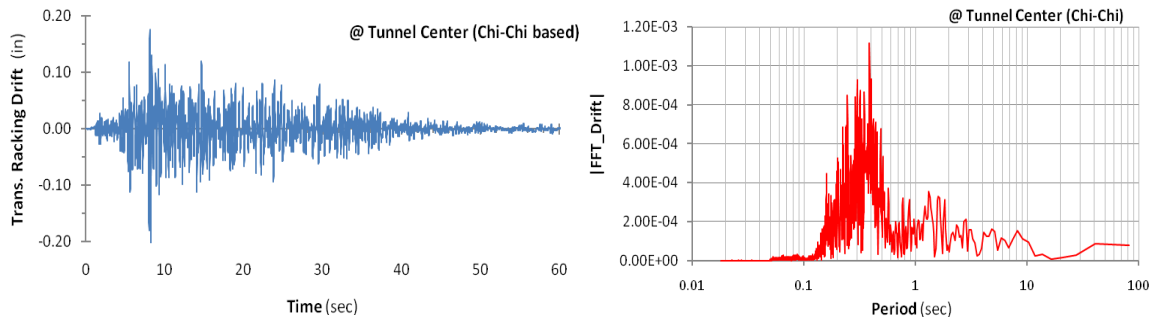
### 3.2.1. Racking Drift Response Distribution

Figure 3.3 shows the distribution of transverse racking drift displacements along the tunnel alignment. The drift distortion induced in the tunnel walls is calculated by the differential horizontal displacement between the crown and the invert, removing displacements due to rigid body rotation of the tunnel cross-section. Note that the peak drift occurs at the west end of the tunnel where the north wall is exposed (see Figure 1.1).



**Figure 3.3.** Transverse racking drift distribution along tunnel for SEE

A sample of the drift time-history response close to the center of the tunnel and its frequency content (Fourier Transform) is shown in Figure 3.4, which clearly shows the effect of the soil-structure frequency band of Figure 3.2.



**Figure 3.4.** 3D SASSI2000 Model transverse racking drift response, close to center (STA 82+00)

An important aspect of the transverse racking drift response is its relationship with the Racking Ratio discussed above. Table 3.1 presents the racking ratios,  $R = \Delta_{SSI} / \Delta_{FF}$ , in the buried portion of the tunnel at several locations along the alignment, based on the data presented in Figure 3.3 and the corresponding free-field racking displacements obtained from the site response analyses. These ratios vary from 3.14 to 5.17 (for different ground motions load cases and along the tunnel alignment), exceed the typical value in the order of 2.75 or so that conventionally used in 2D manual analyses. This result indicates that the 3D SSI effect is significant due to: 3D geometry and loading, kinematic and inertial interaction, and proximity of the adjacent tunnel. A companion parametric study performed (Liu, C. et al, 2012) also indicates that additional amplification of these values (in the order of 30-50%) occur due to the presence of waterproofing membranes that reduce the side-shear resistance between the tunnel and surrounding soil.

**Table 3.1.** Distribution of tunnel cross-section racking drift and Racking Ratios

| STA.  | Manjil-based Motions |                    |                              | Kocaeli-based Motions |                    |                              | Chi-Chi-based Motions |                    |                              |
|-------|----------------------|--------------------|------------------------------|-----------------------|--------------------|------------------------------|-----------------------|--------------------|------------------------------|
|       | $\Delta_{SSI}$ (in)  | $\Delta_{FF}$ (in) | $\Delta_{SSI} / \Delta_{FF}$ | $\Delta_{SSI}$ (in)   | $\Delta_{FF}$ (in) | $\Delta_{SSI} / \Delta_{FF}$ | $\Delta_{SSI}$ (in)   | $\Delta_{FF}$ (in) | $\Delta_{SSI} / \Delta_{FF}$ |
| 76+30 | 0.18                 | 0.05               | 3.64                         | 0.18                  | 0.04               | 4.08                         | 0.19                  | 0.05               | 3.56                         |
| 78+80 | 0.20                 | 0.05               | 4.06                         | 0.20                  | 0.04               | 4.48                         | 0.22                  | 0.05               | 4.07                         |
| 81+00 | 0.25                 | 0.05               | 5.17                         | 0.20                  | 0.04               | 4.47                         | 0.25                  | 0.05               | 4.61                         |
| 84+40 | 0.20                 | 0.05               | 4.13                         | 0.18                  | 0.04               | 4.03                         | 0.17                  | 0.05               | 3.14                         |



### 3.2.3. Internal Stresses & Strains

Longitudinal stresses due to internal loads generated in the walls, roof, and invert slab induced by 3D SSI effects are depicted in Figure 3.5 for two cross section of the lining.

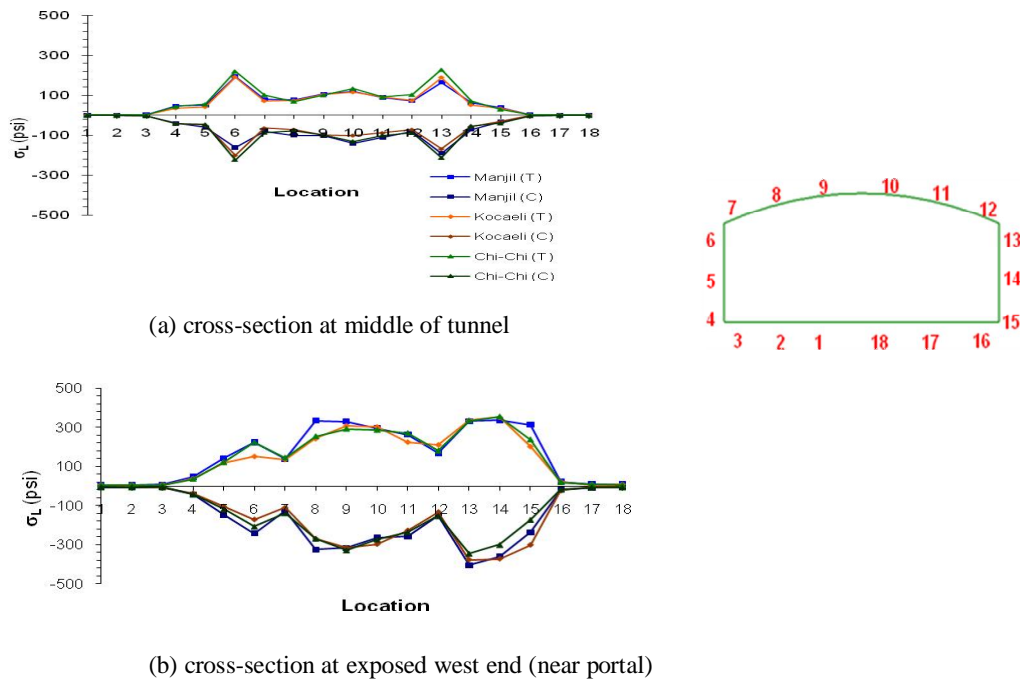


**Figure 3.5.** Longitudinal stress distributions in tunnel lining cross-section

Clearly, these distributions demonstrate the merits of 3D analyses for the determination of stress and more importantly strain distributions (which define damage measures) in the tunnel lining. As shown in the figure, there is considerable difference in the predicted stress level in the tunnel lining between the buried and exposed segments of tunnel. A similar trend exists of the shear stress distribution in the lining.

An order of magnitude comparison of strains obtained with manual calculations based on quasi-static ground-imposed loading shows that the peak normal strain corresponding to the 300 psi stress in Figure 3.5(a),  $\epsilon_n = 1.0 \times 10^{-4}$  using 4,000 psi concrete strength, compares well with the slightly higher value  $\epsilon_{nm} = V_s/2C_s = 1.26 \times 10^{-4}$  computed for particle velocity  $V_s = 25$  in/sec and propagation velocity  $C_s = 2.5$  km/sec of travelling shear waves, using the quasi-static deformation procedure in (Hashash et al, 2001).

## 4. CONCLUSIONS

The use of 3D models for the seismic performance evaluation of large-scale tunnels with curved alignment geometries, in the presence of additional adjacent tunnels, reveals important behaviours that are otherwise difficult to capture by simpler analytic techniques. It is shown that SASSI2000 is a viable tool for the development of tractable models and SSI analyses of complex tunnel structures, notwithstanding the fact that non-homogenous soil profiles and non-linearities (in the soil and structure) cannot be represented directly. However, these effects can be accounted for reasonably well in tunnel soil-structure systems of the type discussed in the case study. Care must be taken in developing the frequency set for the computation of the transfer functions, since the interpolation scheme is sensitive to certain problem types, particularly in the high frequency range.

## AKCNOWLEDGEMENT

The authors wish to thank and acknowledge the project sponsors, San Francisco City and County Transportation Authority (SFCTA) and the California Department of Transportation (Caltrans), as well as our design development team colleagues at Caltrans, Arup, AMEC-Geomatrix, and Parsons Brinckerhoff,.

## REFERENCES

- Ostadan, F. (2006). SASSI2000 A System for Analysis of Soil-Structure Interaction, Revision 2, User's Manual and Theoretical Manual.
- Penzien, J. (2000). Seismically induced racking of tunnel linings. *Earthquake Engineering & Structural Dynamics*. **Vol 29**, pp. 683-691.
- ADINA R & D, Inc. (2005). ADINA Theory and Modeling Guide.
- Itasca Consulting Group Inc. (1998). FLAC: Fast Lagrangian Analysis of Continua.
- Liu, C., R. Donikian, M. Nelson, F. Greguras, and C-Y Chang (2012). Studies on Seismic Design and Performance Assessment of Cut-And-Cover Tunnels. *Submitted to 15<sup>th</sup> World Conference on Earthquake Engineering (15WCEE), Lisbon, Portugal*.
- Hashash, Y.M.A, J.J. Hook, B. Schmidt, and J.I-C. Yao. (2001). Seismic design and analysis of underground structures. *Tunneling and Underground Space Technology, International Tunneling Association*. **Vol 16**, pp. 247-293.